Pergamon

Tetrahedron Vol. 51, No. 26, pp. 7149-7160, 1995

0040-4020/95 $9.50+0.00

0040-4020(95)00364-9

The Absolute Configuration of Trilobacin and Trilobin, A Novel Highly Potent Acetogenin from the Stem Bark of *Asimina triloba* (Annonaceae)

Geng-Xian Zhao, Zhe-Ming Gu, Lu Zeng, Jin-Feng Chao, John F. Kozlowski, Karl V. Wood†, and Jerry L. McLaughlin*

Department of Medicinal Chemistry and Pharmacognosy, School of Pharmacy and Pharmacal Sciences, †Department of Chemistry, School of Sciences, Purdue University, West Lafayette, IN 47907 U.S.A.

Abstract: Trilobacin (**1**) is the only previously reported Annonaceous acetogenin with the *erythro* relative configuration between the adjacent bis-tetrahydrofuran (THF) rings. The relative configuration in the adjacent bis-THF moiety of **1** was corrected to *threo/trans/erythro/cis/threo* from C-15 to C-24, and the absolute configuration was determined as 4*R*, 15*R*, 16*R*, 19*R*, 20*S*, 23*R*, 24*R* and 36*S* by advanced Mosher ester methodology and the COSY and NOESY spectral analyses of its 4,24-diacetate (**1a**). Further investigation of the EtOH extract of the stem bark of the paw paw tree, *Asimina triloba*, monitoring for bioactivity by brine shrimp lethality, led to a novel acetogenin, trilobin (**2**). Spectral and chemical methods identified **2** as a 4-deoxy-10-hydroxy isomer of **1**. The absolute configuration of **2** was determined as 10*R*, 15*R*, 16*R*, 19*R*, 20*S*, 23*R*, 24*R*, and 36*S* by analyses of its Mosher ester derivatives. **2** was selectively cytotoxic among three human solid tumor cell lines with over a billion times the potency of adriamycin.

INTRODUCTION

The Annonaceous acetogenins are endemic to certain plants of the Annonaceae. These polyketide derived natural products have received, in recent years, much interest due to their significant antitumor, antiinfective, and pesticidal activities. More than 160 acetogenins have been reported, to date, from twenty species of six genera in this family.[1-3] Studies on the primary mode of action have now well established that the Annonaceous acetogenins are powerful inhibitors of the NADH-ubiquinone oxidoreductase (Complex I) of mammalian and insect mitochondrial electron transport systems; thus, Annonaceous acetogenins can inhibit ATP production at the cellular level.[4-7] Certain acetogenins are more potent than rotenone and piericidin and could be considered, therefore, the most powerful inhibitors of mitochondrial Complex I reported to date.[7,8] Recent studies have also demonstrated a powerful inhibition of the ubiquinone-linked NADH oxidase that is active in the plasma membranes of tumor cells but not activated in nontumor cells.[9] The consequences of these combined actions may be linked to programmed cell death (apoptosis) and account for their high potencies in various bioassay systems.[10]

Asimina triloba (L.) Dunal, a native North American plant commonly named the paw paw tree, belongs to the Annonaceae. The pesticidal properties of the EtOH extract from its stem bark attracted our interest in the bioactive components, and previous investigations led us to fourteen highly potent Annonaceous acetogenins and four non-acetogenin compounds.[11-15] Among these acetogenins, an interesting finding was trilobacin (**1**) (Figure 1)[12] which has been, until now, the only reported adjacent bis-THF acetogenin having an *erythro* relative configuration between the two adjacent THF rings, and, thus, it represents a new stereochemical type of

adjacent bis-THF subunit.[1-3] Trilobacin (**1**) showed significant cytotoxicities in the brine shrimp lethality test (BST) and in the *in vitro* human cancer cell line tests at NIH/NCI and the Purdue Cancer Center.[12] These bioactivities are quite comparable to its diastereomers, asimicin and bullatacin, two patented pesticidal and chemotherapeutic agents.[1-3] **1** exhibited, interestingly, several times the activity of asimicin and bullatacin against A-549 (human lung cancer, ED_{50}: 1.7 x 10^{-6} μg/ml)) and P-388 (human leukemia, ED_{50}: 2.2 x 10^{-6} μg/ml) cell lines at the Abbott Laboratories.[16] However, the absolute configuration of **1** had not been previously solved.

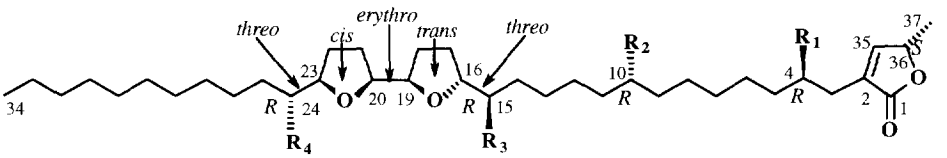

1	R_1=OH	R_2=H	R_3=OH	R_4=OH
1a	R_1=OAc	R_2=H	R_3=OH	R_4=OAc
1b	R_1=OAc	R_2=H	R_3=OTMSi	R_4=OAc
1c	R_1=O-(*S*)-MTPA	R_2=H	R_3=O-(*S*)-MTPA	R_4=O-(*S*)-MTPA
1d	R_1=O-(*R*)-MTPA	R_2=H	R_3=O-(*R*)-MTPA	R_4=O-(*R*)-MTPA
2	R_1=H	R_2=OH	R_3=OH	R_4=OH
2a	R_1=H	R_2=OAc	R_3=OAc	R_4=OAc
2b	R_1=H	R_2=OTMSi	R_3=OTMSi	R_4=OTMSi
2c	R_1=H	R_2=O-(*S*)-MTPA	R_3=O-(*S*)-MTPA	R_4=O-(*S*)-MTPA
2d	R_1=H	R_2=O-(*R*)-MTPA	R_3=O-(*R*)-MTPA	R_4=O-(*R*)-MTPA

Fig. 1. Chemical Structures of Trilobacin (**1**), Trilobin (**2**) and Their Derivatives.

In this paper, we report stereochemical studies, which determine the absolute configuration of trilobacin (**1**), and the isolation and complete structural analysis of trilobin (**2**). The preparation of trilobacin 4,24-diacetate (**1a**) (Figure 1) followed by EIMS, COSY and NOESY spectral analyses established the C-20/C-23 THF ring to have the *cis* configuration and permitted the revision of the relative configuration of **1**,[12] from C-15 to C-24, to *threo/trans/erythro/cis/threo*. Using advanced Mosher's methodology,[17-19] the absolute configuration of **1** was, therefore, determined as 4*R*, 15*R*, 16*R*, 19*R*, 20*S*, 23*R*, 24*R*, and 36*S*. The novel compound, trilobin (**2**), was identified as the second known member of the trilobacin-type acetogenins. **2** was determined to be 4-deoxy-10-hydroxytrilobacin, with a 10*R* configuration; **2** exhibited selective cytotoxic potencies over a billion times those of adriamycin.

RESULTS AND DISCUSSION

Trilobacin (**1**) was described as a new acetogenin from *Asimina triloba* in 1992 (Figure 1). By comparison of its triacetate with model compounds,[3] the relative configuration of **1** was suggested as *threo/trans/erythro/trans/threo*, in the adjacent bis-THF moiety from C-15 to C-24.[12] In order to determine the absolute configuration of **1**, the per-(*R*)- and per-(*S*)-methoxy(trifluoromethyl)phenylacetic acid (MTPA or Mosher ester) derivatives (**1c** and **1d**) (Figure 1) were prepared, and their proton chemical shifts were carefully assigned based on ^{1}H-^{1}H-COSY spectral analyses (Table 1). The ^{1}H-NMR data of the protons around the adjacent bis-THF ring and the γ-lactone ring moieties of **1c** and **1d** are tabulated in Table 2.

The analysis of the $\Delta\delta_H(\delta_S-\delta_R)$ data around the γ-lactone ring moiety showed a negative result for H-5 and positive results on the lactone ring side, i.e., for H-3, H-35, H-36 and H-37 (Table 2). These results are

Table 1. ^{1}H- and ^{13}C-NMR Data (δ) of Trilobacin (**1**) and Its Derivatives **1a**, **1c**, and **1d**.

No. (H/C)	δ_H (500 MHz) (J in Hz)				δ_C (125 MHz)
	1* ($CDCl_3$)	**1a** (C_6D_6)	**1c** ($CDCl_3$)	**1d** ($CDCl_3$)	**1** ($CDCl_3$)
1					174.5
2					131.1
3a	2.53 dddd (15.5, 3.5, 1.5, 1.5)	2.44 dddd (15.5, 3.5, 1.5, 1.5)	2.56 dddd (15.5, 3.5, 1.5, 1.5)	2.61 dddd (15.5, 3.5, 1.5, 1.5)	33.4
3b	2.40dddd (15.5, 8, 1.5, 1.5)	2.35 ddd (15.5, 8, 1.5, 1.5)	2.61 dddd (15.5, 8, 1.5, 1.5)	2.68 dddd (15.5, 8, 1.5, 1.5)	
4	3.83 m	5.20 m	5.32 m	5.38 m	70.0
5	1.49 m	1.48 m	1.67 m	1.65 m	37.4
6	1.22-1.54 m	1.2-1.52 m	1.2-1.7 m	1.1-1.7 m	25.6**
7-12	1.22-1.54 m	1.2-1.52 m	1.2-1.7 m	1.1-1.7 m	**
13	1.22-1.54 m	1.2-1.52 m	1.2-1.7 m	1.1-1.7 m	25.7**
14	1.41 m	1.51 m	1.61 m	1.46 m	33.6
15	3.36 ddd (8, 5, 5)	3.38 m	5.03 m	5.05 m	74.6
16	3.83 m	3.85 m	3.93 ddd (6.5, 6.5, 6.5)	3.94 ddd (6.5, 6.5, 6.5)	83.3
17a	1.96m	1.74 m	1.79 m	1.91 m	***
17b	1.74 m	1.44 m	1.47 m	1.58 m	
18a	1.94 m	1.72 m	1.80 m	1.97 m	25.9**
18b	1.86 m	1.65 m	1.66 m	1.80 m	
19	3.97 ddd (7, 6.5, 5)	3.70 m	3.63 ddd (6.5, 6.5, 6.5)	3.79 ddd (6.5, 6.5, 6.5)	81.6
20	4.05 ddd (8.5, 6, 5)	3.85 m	3.71 ddd (6.5, 6.5, 6.5)	3.75 ddd (6.5, 6.5, 6.5)	80.9
21a	2.05 m	1.72 m	1.76 m	1.99 m	25.8**
21b	1.70 m	1.65 m	1.48 m	1.66 m	
22a	1.96 m	1.75 m	1.90 m	1.95 m	27.1
22b	1.74 m	1.44 m	1.50 m	1.58 m	
23	3.83 m	4.02 m	3.97 ddd (6.5, 6.5, 6.5)	3.98 ddd (6.5, 6.5, 6.5)	82.6
24	3.39 ddd (6.5, 7, 6)	5.10 m	5.03 m	5.05 m	73.9
25	1.41 m	1.53 m	1.61 m	1.46 m	34.2
26	1.22-1.54 m	1.2-1.52 m	1.2-1.7 m	1.1-1.7 m	25.6**
27-31	1.22-1.54 m	1.2-1.52 m	1.2-1.7 m	1.1-1.7 m	***
32	1.22-1.54 m	1.2-1.52 m	1.2-1.7 m	1.1-1.7 m	31.9
33	1.22-1.54 m	1.2-1.52 m	1.2-1.7 m	1.1-1.7 m	22.7
34	0.878 t (7)	0.91 t (7)	0.88 t (7)	0.885 t (7)	14.2
35	7.19 ddd (1.5, 1.5, 1.5)	6.24 ddd (1.0, 1.0, 1.0)	6.73 br	6.97 br	151.7
36	5.06 qddd (7, 1.5, 1.5, 1.5)	4.22 qddd (7, 1.5, 1.5, 1.5)	4.86 qddd (7, 1.5, 1.5, 1.5)	4.91 qddd (7, 1.5, 1.5, 1.5)	78.0
37	1.44 d (7)	0.79 d (7)	1.28 d (7)	1.31 d (7)	19.2
C_4-Ac		1.71 s			
C_{24}-Ac		1.81 s			

* Reassignments are made based on the spectral analysis with TMS as internal reference; $CHCl_3$ was previously used as the internal reference.[12]

** Assignments may be interchanged within the column.

*** The methylene signals are at δ 28.2, 28.3, 29.0, 29.4, 29.5, 29.6, 29.7, and 29.8.

identical to those of the related protons of asimicin and bullatacin as previously described,[17] suggesting that C-4 has the *R* configuration based on the Mosher assumptions.[20-22] The absolute configuration at C-36 in the butenolide ring has been directly determined as *S* only for uvaricin[23] and squamocin.[24-26] However, all acetogenins are predicted as having the 36*S* (or 34*S* in the thirty-five carbon acetogenins) configuration by comparisons of NMR data of the diagnostic protons and carbons with those of uvaricin and squamocin.[1-3] Recently, a novel use of Mosher ester data for determining the relative configuration between C-4 and C-36 of the 4-hydroxylated Annonaceous acetogenins has been described by Hoye et al.[18,19] Analysis of the ^{1}H-NMR data of **1c** and **1d**, using Hoye's new method, indicated that the $|\Delta\delta|$ values for H-35 and H-36 were 0.24 ppm and 0.05 ppm, respectively (Table 2), and strongly suggested an "unlike" relative configuration between C-4 and C-36 for trilobacin (**1**). Since C-4 in **1** has the *R* configuration, C-36 must possess the *S* configuration, as is usual. **1** showed a negative Cotton effect at 235 nm (MeOH, ε=-425) in the CD spectrum which provided further evidence for the 36*S* configuration.[26]

Table 2. Chemical Shift Data (δ) of Relevant Protons of the Per-(***S***)- and (***R***)-MTPA Ester Derivatives of Trilobacin (**1c** and **1d**).

MTPA Config.	Proton Chemical Shifts (δ_H)															
	γ-Lactone Ring Moiety					Adjacent Bis-THF Moiety										
	H-5	H-3	H-35	H-36	H-37	H-14	H-16	H-17	H-18	H-19	H-20	H-21	H-22	H-23	H-25
S	1.67	2.56/ 2.61	6.73	4.86	1.28	1.61	3.93	1.79 /1.47	1.80 /1.66	3.63	3.71	1.76 /1.48	1.90 /1.50	3.97	1.61
R	1.65	2.61 /2.68	6.97	4.91	1.31	1.46	3.94	1.91 /1.58	1.97 /1.80	3.79	3.75	1.99 /1.66	1.95 /1.58	3.98	1.46
$\Delta\delta_H$ (δ_S-δ_R)	+0.02	-0.05 /-0.07	-0.24	-0.05	-0.03	+0.15	-0.01	-0.12 /-0.11	-0.17 /-0.14	-0.16	-0.04	-0.23 /-0.18	-0.05 /-0.08	-0.01	+0.15
Carbinol Config.	C-4***R*** C-36***S***					C-15***R*** C-24***R***										

The $\Delta\delta_H$ (δ_S-δ_R) values of diagnostic protons, in the adjacent bis-THF moiety from C-15 to C-24 of the Mosher ester derivatives, **1c** and **1d**, showed a positive value on the aliphatic chain side (H-14 and H-25) and a negative value on the THF ring side (H-16 to H-23) (Table 2). According to Mosher's configurational correlation model we can assign, unambiguously, the *R* configuration for both C-15 and C-24.[20] However, one of these carbinol centers of **1** must have the *S* configuration if the previously suggested relative stereochemical relationships, *threo/trans/erythro/trans/threo* ,[12] between the chiral centers from C-15 to C-24, were correct. Reexamination of the ^{1}H-NMR and COSY spectra of trilobacin (**1**) and its triacetate derivative confirmed the *erythro* configuration between C-19/C-20 and the *threo* configuration between C-15/C-16 and C-23/C-24. Therefore, it was concluded that one of the THF rings had the *cis* relative configuration and the other had the *trans* configuration. To confirm this and determine the location of the *cis* THF ring, a diacetate derivative of **1**, with one of the flanking hydroxyl groups acetylated (at C-15 or C-24), was required in order to separate all of the methine proton signals of the adjacent bis-THF moiety; these signals are overlapped in the region from δ 3.36 to 4.05 in the ^{1}H-NMR spectrum (Table 1). For this purpose, the acetylation of **1** was carefully controlled and monitored by thin-layer chromatography. The product mixture was subjected to high performance liquid chromatographic (HPLC) separation and yielded trilobacin-4,24-diacetate (**1a**) (Figure 1). The location of the free hydroxyl group at the C-15 position in **1a** was determined by the diagnostic fragment ion at m/z 425 (Figure 2) which was the base peak in the EIMS spectrum of the TMSi derivative (**1b**) (Figure 1); this was further confirmed by HR-EIMS measurement of the peak at m/z 425.2714 corresponding to the fragment $C_{23}H_{41}O_5Si$ (calcd 425.2723). The assignment of all the proton signals in the ^{1}H-NMR spectrum (in C_6D_6) of **1a** was made by careful analysis of its ^{1}H-^{1}H COSY spectrum as listed in Table 1.

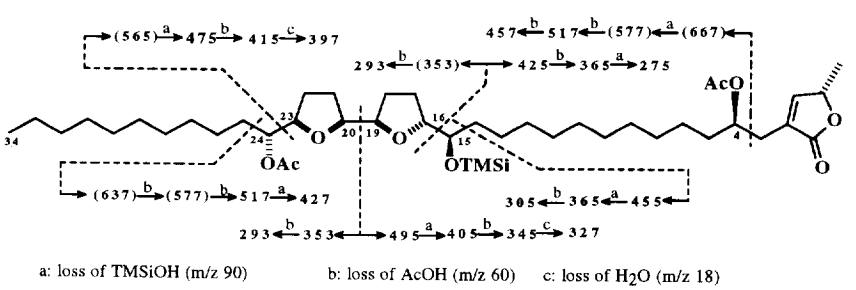

Fig. 2. Diagnostic EIMS Data of the Trilobacin-4,24-Diacetate-15-TMSi Derivative (**1b**).

As shown in Figure 3, strong NOE effects were observed between H-19/H-20 and H-20/H-23 in the NOESY spectrum of **1a**, and weak NOE effects between H-23/H-19 and H-19/H-15 occurred as smaller cross peaks due to their long range 'through space' interactions. Therefore, it was concluded that the *cis* -THF ring is located between C-20 and C-23, while the *trans* configuration is between C-16 and C-19. The relative configuration of the bis-THF system of **1** was then revised to *threo/trans/erythro/cis/threo* from C-15 to C-24. Moreover, using the Mosher ester data, the absolute configuration of **1** can be summarized as 4*R*, 15*R*, 16*R*, 19*R*, 20*S*, 23*R*, 24*R*, and 36*S* as shown in Figure 1. Based on these results all of the proton and carbon resonances of **1** were reassigned and presented in Table 1.

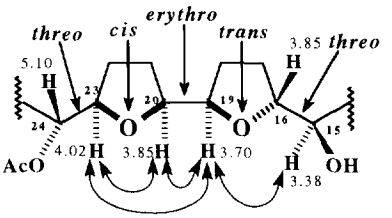

Fig. 3. NOE Effects Between Relevant Protons Observed in the NOESY Spectrum of Trilobacin-4,24-Diacetate (**1a**).

Trilobin (**2**) (Figure 1) was isolated as a white wax. The prominent molecular adduct peaks at m/z 623 (MH^+) and 645 (MNa^+) in the FABMS (glycerol) of **2** indicated the molecular weight of 622. This was confirmed by its HR-FABMS (glycerol) spectrum in which the molecular ion peak was found at m/z 623.4841 (MH^+) and matched the exact mass 623.4887 calculated for the molecular formula $C_{37}H_{66}O_7$. Analyses of the UV, IR, ^{1}H-, and ^{13}C-NMR spectra of **2** and comparisons of these spectral data with those of trilobacin (**1**) suggested that **2** belongs to the trilobacin-type of adjacent bis-THF acetogenins. The presence of a 4-deoxy-γ-lactone terminal was clearly indicated by the proton resonances at δ 2.27 (H-3), 6.99 (H-35), 5.00 (H-36), and 1.42 (H-37) in the ^{1}H-NMR spectrum (Table 3), and the carbon signals at δ 25.2 (C-3), 134.3 (C-2), 148.9 (C-35), 77.4 (C-36), and 19.2 (C-37) in the ^{13}C-NMR spectrum of **2** (Table 3).[1-3] The C-1 (C=O) signal was difficult to record in the ^{13}C-NMR spectrum because of its long relaxation time and the limited amount of sample. To solve this problem the HMBC 2D-NMR technique was applied, and two cross peaks were observed between δ 173.8 and 6.99, and between δ 173.8 and 2.27, due to the coupling of C-1 with H-35 and H-3, respectively. Thus, the chemical shift of C-1 was assigned at δ 173.8. The UV (225 nm, ε=2695) and IR (1756 cm^{-1}) spectral data also supported the presence of the γ-lactone moiety. These data are identical to those of numerous previously reported 4-deoxy-acetogenins.[13,14]

The existence in **2** of an adjacent bis-THF moiety, bearing two flanking hydroxyl groups, was obvious by the diagnostic proton signals in the region from δ 3.36 to 4.05 (Table 3) in the ^{1}H-NMR spectrum and the carbon resonances at δ 74.6 (C-15), 83.2 (C-16), 81.6 (C-19), 80.9 (C-20), 82.6 (C-23), and 73.8 (C-24) in the ^{13}C-NMR spectrum (Table 3); these were essentially identical to those of trilobacin (**1**). The typical proton signals located at δ 3.97 and 4.05 (Table 3) indicated the *erythro* relative configuration between the two adjacent bis-THF rings (H-19 and H-20), as has only been found in the natural trilobacin-type acetogenins.[1] The relative stereochemistry between the carbinol centers in the adjacent bis-THF moiety was determined to be the same as in trilobacin (**1**), i.e., *threo/trans/erythro/cis/threo*, from C-15 to C-24, by ^{1}H-NMR spectral analysis (Table 3)

Table 3. ^{1}H- and ^{13}C-NMR Data (δ) of Trilobin (**2**) and Its Derivatives **2a**, **2c**, and **2d**.

No.	δ_H (500 MHz, $CDCl_3$, J in Hz)				δ_C (125 MHz, $CDCl_3$)
(H/C)	**2**	**2a**	**2c**	**2d**	**2**
1					173.8
2					134.3
3	2.27 t (7.5)	2.27 t (7.5)	2.256 t (7.5)	2.249 t (7.5)	25.2
4	1.54 m	1.54 m	1.54 m	1.51 m	27.4
5-7	1.22-1.60 m	1.24-1.64 m	1.2-1.7 m	1.1-1.7 m	**
8	1.22-1.60 m	1.22-1.64 m	1.2-1.7 m	1.1-1.7 m	25.7*
9	1.43 m	1.57 m	1.61 m	1.46 m	37.4
10	3.59 m	4.85 m	5.0 m	5.05 m	71.9
11	1.43 m	1.57 m	1.61 m	1.46 m	37.4
12, 13	1.22-1.60 m	1.22-1.64 m	1.2-1.7 m	1.1-1.7 m	**
14	1.41 m	1.57 m	1.61 m	1.46 m	33.5
15	3.36 m	4.85 m	5.0 m	5.05 m	74.6
16	3.83 m	3.94 ddd (7, 6.5, 5)	3.92 m	3.94 ddd (6.5, 6.5, 6.5)	83.2
17a	1.96m	1.96 m	1.79 m	1.91 m	**
17b	1.74 m	1.58 m	1.47 m	1.58 m	
18a	1.94 m	1.92 m	1.80 m	1.97 m	25.7*
18b	1.86 m	1.75 m	1.66 m	1.80 m	
19	3.97 ddd (7, 6.5, 5)	3.84 m	3.63 m	3.79 ddd (6.5, 6.5, 6.5)	81.6
20	4.05 ddd (8.5, 6, 5)	3.84 m	3.71 m	3.75 ddd (6.5, 6.5, 6.5)	80.9
21a	2.05 m	1.92 m	1.76 m	1.99 m	25.8*
21b	1.70 m	1.75 m	1.48 m	1.66 m	
22a	1.96 m	1.99 m	1.90 m	1.95 m	27.0
22b	1.74 m	1.68 m	1.50 m	1.58 m	
23	3.83 m	3.98 ddd (8.5, 6, 5)	3.97 m	3.98 ddd (6.5, 6.5, 6.5)	82.6
24	3.40 m	4.85 m	5.0 m	5.05 m	73.8
25	1.41 m	1.57 m	1.61 m	1.46 m	34.3
26	1.22-1.60 m	1.22-1.64 m	1.2-1.7 m	1.1-1.7 m	25.6*
27-31	1.22-1.60 m	1.22-1.64 m	1.2-1.7 m	1.1-1.7 m	**
32	1.22-1.60 m	1.22-1.64 m	1.2-1.7 m	1.1-1.7 m	31.9
33	1.22-1.60 m	1.22-1.64 m	1.2-1.7 m	1.1-1.7 m	22.7
34	0.878 t (7)	0.88 t (7)	0.88 t (7)	0.88 t (7)	14.1
35	6.99 ddd (1.5, 1.5, 1.5)	6.99 ddd (1.0, 1.0, 1.0)	6.98 br	6.98 ddd (1.5, 1.5, 1.5)	148.9
36	5.0 qddd (7, 1.5, 1.5, 1.5)	5.0 qddd (7, 1.5, 1.5, 1.5)	5.0 m	5.0 m	77.4
37	1.42 d (7)	0.1.41 d (7)	1.40 d (7)	1.40 d (7)	19.2
C_{10}-Ac		2.04 s			
C_{15}-Ac		2.08 s			
C_{24}-Ac		2.08 s			

* Assignments may be interchanged within the column.

** The methylene signals are at δ 28.2, 28.9, 29.1, 29.3, 29.5, 29.6, and 29.7.

and comparison of the NMR data of the triacetate derivative (**2a**) with those of model compounds[27,28] and trilobacin triacetate.[12] The FABMS of **2** suggested the presence of three hydroxyl groups in the molecule, showing ions at m/z 605, 587, and 569 arising from successive losses of three H_2O molecules (m/z 18) from the molecular ion (MH^+, m/z 623) (Figure 4). This assumption was supported by the successive losses of three TMSi-OH molecules (m/z 90), showing at m/z 748, 658, and 568, from the molecular ion (M^+, m/z 838) in the EIMS spectrum of its tri-TMSi derivative (**2b**) (Figures 1 and 4). Moreover, the three acetate methyl resonances at δ 2.04 (3H) and 2.08 (6H) in the ^{1}H-NMR spectrum of **2a** provided further evidence for three hydroxyl groups (Table 3). It was concluded that in addition to the two hydroxyl groups flanking the bis-THF system, there was a third hydroxyl located somewhere in the aliphatic chain. This conclusion was supported by the multiple proton peak at δ 3.59 in the ^{1}H-NMR spectrum (Table 3). The positions of the adjacent bis-THF moiety and the three hydroxyl groups were determined by the EIMS spectrum of the tri-TMSi derivative (**2b**). As shown in Figure 4, the EIMS diagnostic fragment ions of **2b** clearly illustrated that the bis-THF unit was situated from C-16 to C-23 and its two flanking hydroxyls were at C-15 and C-24, as found in trilobacin (**1**).

The third hydroxyl was predicted to be located at the C-10 position in **2** by the critical mass fragment ion at m/z 225 (Figure 4), and this was confirmed in the HR-EIMS of **2b** through the observation of the ion peak at m/z 297.1880 corresponding to $C_{16}H_{29}O_3Si$ (calcd 297.1886).

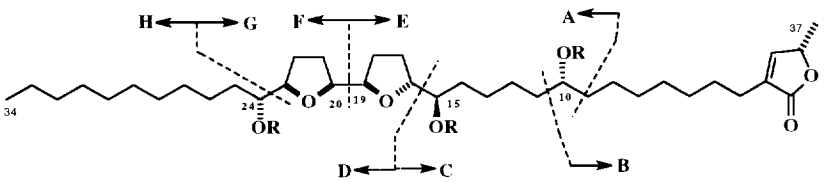

R	M^+/MH^+	A	B	C	D	E	F	G	H
H (**2**)	623	(427)	225	311	311	(381)	241		
(EIMS)	605 (a)	409 (a)		293 (a)	293 (a)	363 (a)	223 (a)		
(FABMS)	587 (a)	391 (a)		275 (a)		345 (a)	205 (a)		
	569 (a)	373 (a)							
TMSi	838	643	297	455	383	525	313	595	243
(**2b**)	748 (b)	553 (b)		365 (b)		435 (b)		505 (b)	
(EIMS)	658 (b)			275 (b)				415 (b)	
	568 (b)							397 (b)	

(a): loss of H2O (m/z 18) (b): loss of TMSi-OH (m/z 90)

Fig. 4. Diagnostic EIMS and FAB-MS Fragment Ions of Trilobin (**2**) and Its tri-TMSi Derivative (**2b**).

The absolute configuration of **2** was determined by Mosher ester methodology through the analyses and comparisons of ^{1}H-NMR spectra of the per-(*S*)-MTPA and per-(*R*)-MTPA derivatives (**2c** and **2d**) (Figure 1, Tables 3 and 4). The $\Delta\delta_H$ values, showing positive values on the chain side and negative values on the ring side in the adjacent bis-THF moiety, indicated the *R* configuration at both C-15 and C-24 (Table 4). The C-10 hydroxyl was located in the middle of the aliphatic chain, and the chemical shifts of its adjacent methylene protons (H-9 and H-10) could not be distinguished by means of up to date NMR techniques. Moreover, direct observation of the magnitude of chemical shift changes of these protons was impossible due to the overlapping of their correlation signals themselves and with those of H-14 and H-25 in the COSY spectra of both MTPA esters. The chemical shifts of H-14 and H-15 could not be used because the diamagnetic effects of the Mosher residues at C-10 on these protons were much weaker than those of the Mosher residues at C-15 and C-24, and also these proton resonances were overlapped with those of H-24 and H-25 in their 1D and 2D NMR spectra. The only signals that could be used are those of the protons on the lactone ring side. The nearest assignable resonances are H-4 and H-3 which are six and seven bonds away from C-10, respectively. The $\Delta\delta_H$ values of two methyl groups of the (*R*)-MTPA ester of the model compounds, 6-undecanol and 8-pentadecanol, were diagnostic (0.039 ppm and 0.007 ppm) and useful for the prediction of the absolute stereochemistry of a carbinol center located six and seven bonds away from the observed protons.[29] The chemical shifts of H-4 and H-3 of the two MTPA derivatives (**2c** and **2d**) showed the expected diagnostic differences, i.e., the δ_S-δ_R values were +0.03 ppm (15 Hz) and +0.007 ppm (3.5 Hz), respectively (Table 4). Similar results were observed in the determination of the absolute configuration at C-10 of asimin (10*R*-hydroxy-4-deoxyasimicin) and bullatin (10*S*-hydroxy-4-deoxybullatacin). Thus, the *R* configuration was proposed at the C-10 position of **2**. All of the proton NMR data listed in Tables 1 and 2 were collected at 500 MHz by modern 2D NMR techniques[17,20] which permit the identification of minor chemical shift differences within the digital resolution of 0.06 Hz per point in ^{1}H-NMR spectra and less than 4 Hz per point in ^{1}H-^{1}H COSY spectra.

Table 4. Chemical Shift Data of Relevant Protons of the Per-(*S*)- and (*R*)-MTPA Ester Derivatives of Trilobin (**2c** and **2d**).

MTPA Config.	Proton Chemical Shifts (δ_H)											
	C-10		Adjacent Bis-THF Moiety									
	H-4	H-3	H-14	H-16	H-17	H-18	H-19	H-20	H-21	H-22	H-23	H-25
S	1.54	2.256	1.61	3.97	1.79 /1.47	1.80 /1.66	3.64	3.72	1.76 /1.48	1.90 /1.50	3.92	1.61
R	1.51	2.249	1.46	3.98	1.91 /1.58	1.97 /1.80	3.79	3.75	1.99 /1.66	1.95 /1.58	3.94	1.46
$\Delta\delta_H$ (δ_S-δ_R)	+0.03	+0.007	+0.15	-0.01	-0.12 /-0.11	-0.17 /-0.14	-0.15	-0.03	-0.23 /-0.18	-0.05 /-0.08	-0.02	+0.15
Carbinol Config.	C-10*R*		C-15*R*						C-24*R*			

The new Mosher ester method of Hoye et al.[18,19] is not applicable to the determination of the absolute configuration of C-36 in **2** due to the absence of the C-4 hydroxyl group. However, a negative Cotton effect at 236 nm in the CD spectrum of squamocin is attributable to the 36*S* configuration in the γ-lactone moiety and provides an useful method for the determination of the C-36 configuration in other Annonaceous acetogenins.[26] A negative Cotton effect at 233 nm in the CD spectrum of **2** was observed; comparing with squamocin (which has a negative Cotton effect at 235 nm in our laboratory), **2** is, therefore, depicted as having the 36*S* configuration. Thus, the structure of trilobin (**2**) was established as illustrated (Figure 1); **2** is the second member of the trilobacin-type of adjacent bis-THF acetogenins and is 10*R*-hydroxy-4-deoxytrilobacin.

Trilobin (**2**) exhibited significant activities in the brine shrimp lethality test[30,31] and in human solid tumor cytotoxicity tests against the lung cancer (A-549), breast cancer (MCF-7), and colon cancer (HT-29) cell lines, with ED_{50} values as low as 10^{-12} μg/ml (Table 5). **2** was, selectively, from one million to nearly ten billion times the cytotoxic potency of the standard reference, adriamycin. These activities are quite comparable to those of trilobacin (**1**) and the asimicin and the bullatacin series of acetogenins.[12-14]

Table 5. Bioactivity Data of Trilobacin (**1**) and Trilobin (**2**)

Compounds	BST[a] LC_{50} (μg/ml) (95% Confidence interval)	Human Cancer Cell Lines (ED_{50} μg/ml)		
		A-549[b]	MCF-7[c]	HT-29[d]
trilobacin (**1**)[e]	8.7×10^{-3} (5.2×10^{-3}-14.4×10^{-3})	8.02×10^{-4}	3.39×10^{-1}	$< 10^{-12}$
trilobin (**2**)	9.7×10^{-3} (5.3×10^{-3}-1.62×10^{-2})	5.71×10^{-12}	2.95×10^{-12}	2.20×10^{-8}
adriamycin[f]	2.57×10^{-1} (1.89×10^{-1}-5.3×10^{-1})	1.84×10^{-2}	1.32×10^{-1}	3.60×10^{-2}

[a] BST: brine shrimp test [b] A-549: human lung cancer [c] MCF-7: human breast cancer
[d] HT-29: human colon cancer [e] data taken from ref. 12. [f] standard reference antitumor compound

EXPERIMENTAL

General Experimental Procedures

Optical rotations were taken on a Perkin-Elmer 241 polarimeter. IR spectra were obtained on a Perkin-Elmer 1600 FTIR spectrometer. UV spectra were measured on a Beckman DU-7 UV spectrometer. CD spectra

were performed on a JASCO Model J600 Circular Dichroism Spectropolarimeter. ^{1}H-NMR and ^{13}C-NMR spectra were recorded on a Varian VXR-500S (^{1}H at 500 MHz, ^{13}C at 125.75 MHz) spectrometer in $CDCl_3$ and C_6D_6 with proton signals referenced to TMS and carbon resonances referenced to $CDCl_3$. Low resolution CIMS and EIMS data were collected on a Finnigan 4000 spectrometer. FABMS, EIMS for TMSi derivatives and exact mass measurements through peak matching were performed on a Kratos MS50 mass spectrometer.

Chromatography

TLC separations were made on Si gel 60 F-254 (EM5717) glass plates (0.25 mm) and visualized by spraying with 5% phosphomolybdic acid in EtOH and heating. Chromatotron plates (1 or 2 mm) were prepared with silica gel 60 PF 254 containing gypsum and dried at 70^{0} overnight. HPLC was carried out with a Rainin HPLC instrument using the Dynamax software system and silica gel columns (a 21.4 mm I.D. x 250 mm column and a 4.6 mm I.D. x 250 mm column) equipped with a Rainin UV-1 detector set at 230 nm.

Plant Material

The stem bark of *Asimina triloba* (L.) Dunal (Annonaceae) was collected from stands growing wild at the Purdue Horticultural Research Farm, West Lafayette, Indiana. The identification was confirmed by Dr. George R. Parker, Department of Forestry and Natural Resources, Purdue University. A voucher specimen of the bark is preserved in the pharmacognosy herbarium.

Bioassays

The extracts, fractions, and isolated compounds were routinely evaluated for lethality to brine shrimp larvae (BST) as described and modified.[30,31] Seven-day *in vitro* MTT cytotoxicity tests against human tumor cell lines were carried out at the Purdue Cancer Center, using standard protocols for A-549 (human lung carcinoma), MCF-7 (human breast carcinoma), and HT-29 (human colon adenocarcinoma) with adriamycin as a positive control.

Extraction, Isolation, and Purification

The extraction procedures were the same as those described in our previous reports.[12-15] The most bioactive fraction, F005 (BST LC_{50} 7.151×10^{-1} µg/ml) (200 g) was applied to an open column on silica gel (8 Kg, 60-200 mesh), eluting with hexane-EtOAc and EtOAc-MeOH gradients; 12 pools were made from the collected fractions according to their TLC patterns and evaluated by the BST bioassay. The very active pools, 5-7 (35 g in total), were combined and further separated by column chromatography (silica gel, 1000 g, 230-400 mesh), using a gradient of an acetone-hexane system, and 88 fractions of 200 ml each were collected. The mother liquor of bioactive fractions, 72-88, from which asimicin, bullatacin, and trilobacin (**1**) were isolated,[12] was concentrated and further resolved by silica gel HPLC columns, eluted with 10%THF in MeOH-hexane gradients (5-12%) and MeOH in $CHCl_3$ (0-1.5%), to yield compound **2**.

Preparation of TMSi derivatives

N, O-bis-(Trimethylsilyl)-acetamide (BSA) and pyridine in silylation grade were purchased from Pierce Chemical Company (USA). TMSi derivatives were prepared by treatment of the isolated acetogenins with BSA in the presence of pyridine. Approximately 300 µg of pure compound was placed in a 100 µl conical reaction vial and dried in a vacuum desiccator over P_2O_5 for 24 hrs. The sample was treated with 2 µl pyridine and 20

μl of BSA and heated at 70 °C for 30 min. The EIMS measurements of the derivatives were carried out at a resolution of 1500, scanning mass 900-100 at 30 sec/decade.

Preparation and purification of Mosher esters

The isolated acetogenin (0.5-1 mg of **1** or **2** in 0.3 ml of CH_2Cl_2) was sequentially treated with pyridine (0.2 ml), 4-(dimethylamino)pyridine (0.5 mg), and 25 mg of (*R*)-(-)-α-methoxy-α-(trifloromethyl)-phenylacetyl chloride. The mixture was stirred at room temperature for 4 hours, monitored by TLC, and then passed through a silica gel open column (0.6 x 6 cm), in a disposable pipet, and eluted with 3 ml of CH_2Cl_2 which was dried under a vacuum. The residue was dissolved in CH_2Cl_2 and washed with 1% $NaHCO_3$ (5 ml) and H_2O (2 x 5 ml); the organic layer was dried under vacuum to give the per-(*S*)-Mosher ester derivative. The per-(*R*)-Mosher ester was prepared by using (*S*)-(-)-α-methoxy-α-(trifloromethyl)-phenylacetyl chloride as the reagent. 1D ^{1}H-NMR spectra were recorded in $CDCl_3$ at 500 MHz with data size of 128K and spectral width of 8 ppm (digital resolution: 0.06 Hz per point). 2D ^{1}H-^{1}H COSY spectra were recorded in $CDCl_3$ at 500 MHz with both F1 and F2 data size of 2048 and spectral width of 8 ppm (digital resolution: < 4 Hz per point).

Trilobacin-4,24-diacetate (**1a**)

Compound **1** (2.5 mg) was treated with 1 ml of pyridine and 10 mg of Ac_2O, at room temperature, for four hours and monitored by TLC examination. The product mixture was concentrated and dried, and the residue was purified by HPLC, using a silica gel Dynamax-60A column (4.6 mm I.D. x 250 mm) as the stationary phase and MeOH (containing 10% THF)-hexane (0-5%) as the mobile phase, to afford the trilobacin-4,24-diacetate (**1a**) (0.3 mg) as a colorless wax. ^{1}H-NMR (500 MHz, C_6D_6, TMS reference): see Table 1. Accurate proton assignments were made by the analysis of its ^{1}H-^{1}H COSY spectrum.

Trilobacin-4,24-diacetate-15-TMSi (**1b**)

Compound **1a** (0.3 mg) was treated with BSA and subsequent workup afforded the trilobacin-4,24-diacetate-15-TMSi derivative (**1b**). EIMS: see Fig. 2.; HR-EIMS: m/z found 425.2714, calcd for $C_{23}H_{41}O_5Si$ (425.2723).

Trilobacin-4,15,24-tri-(S)-MTPA ester (**1c**)

Compound **1** (1 mg) was treated with (*R*)-(-)-α-methoxy-α-(trifloromethyl)-phenylacetyl chloride and subsequent workup gave derivative **1c** as a light yellow oil. ^{1}H-NMR (500 MHz, $CDCl_3$, TMS reference): see Table 1. Proton assignments were made by the analysis of its ^{1}H-^{1}H COSY spectrum.

Trilobacin-4,15,24-tri-(R)-MTPA ester (**1d**)

Compound **1** (1 mg) was treated with (*S*)-(-)-α-methoxy-α-(trifloromethyl)-phenylacetyl chloride and subsequent workup gave derivative **1d** as a light yellow oil. ^{1}H-NMR (500 MHz, $CDCl_3$, TMS reference): see Table 1. Proton assignments were made by the analysis of its ^{1}H-^{1}H COSY spectrum.

Trilobin (**2**)

Colorless wax (4 mg), $[\alpha]_D^{22}$: +33.3° (c 0.00015 g/ml, MeOH). UV_{max}^{EtOH} 225 nm (ε=2695); CD (MeOH) ε (nm): -1251 (233); IR (film, CH_2Cl_2) ν_{max} cm^{-1} 3447 (OH), 2927, 2850, 1756 (C=O), 1457,

1375, 1317, 1067, 951; FABMS m/z 623 (MH^+), 605 (MH^+-H_2O), 569 (MH^+-$3H_2O$), 551, 543, 437; HR-FABMS m/z found 623.4841, calcd for $C_{37}H_{67}O_7$ (623.4887, MH^+); EIMS: see Fig. 4.; ^{1}H-NMR (500 MHz, $CDCl_3$, TMS reference): see Table 3. Proton assignments were made by the analysis of its ^{1}H-^{1}H COSY spectrum. ^{13}C-NMR (125 MHz, $CDCl_3$, TMS reference): see Table 3.

Trilobin triacetate (**2a**)

A sample of **2** (0.5 mg) was treated with Ac_2O/pyridine (1:1), at room temparature overnight, and subsequent workup afforded the triacetate (**2a**) as a light yellow wax. ^{1}H-NMR (500 MHz, $CDCl_3$, TMS reference): see Table 3. Proton assignments were made by the analysis of its ^{1}H-^{1}H COSY spectrum.

Trilobin-tri-TMSi (**2b**)

Compound **2** (0.3 mg) was treated with BSA and subsequent workup afforded the tri-TMSi derivative (**2b**). EIMS: see Fig. 4.; HR-EIMS: m/z found 297.1880, calcd for $C_{23}H_{41}O_5Si$ (297.1886).

Trilobin-10,15,24-tri-(S)-MTPA ester (**2c**)

Compound **2** (0.5 mg) was treated with (*R*)-(-)-α-methoxy-α-(trifloromethyl)-phenylacetyl chloride to give **2c** as a light yellow oil. ^{1}H-NMR (500 MHz, $CDCl_3$, TMS reference): see Table 3. Proton assignments were made by the analysis of its ^{1}H-^{1}H COSY spectrum.

Trilobin-10,15,24-tri-(R)-MTPA ester (**2d**)

Compound **2** (0.5 mg) was treated with (*S*)-(-)-α-methoxy-α-(trifloromethyl)-phenylacetyl chloride to give **2d** as a light yellow oil. ^{1}H-NMR (500 MHz, $CDCl_3$, TMS reference): see Table 3. Proton assignments were made by the analysis of its ^{1}H-^{1}H COSY spectrum.

ACKNOWLEDGMENTS

This investigation was supported by grant no. R01 CA 30909 from the National Cancer Institute, NIH. Thanks are due to the Cell Culture Laboratory, Purdue Cancer Center, for the in house cytotoxicity data.

REFERENCES

1. Gu, Z.-M.; Zhao, G.-X.; Oberlies, N. H.; Zeng, L.; McLaughlin, J. L. "Recent Advances in Phytochemistry"; Romeo, J. T. Ed.; Plenum Press: New York, Vol. 29, **1995**; (accepted for publication).
2. Fang, X.-P.; Rieser, M. J.; Gu, Z.-M.; Zhao, G.-X.; McLaughlin, J. L. *Phytochem. Anal.* **1993**, *4*, 27-48 and 49-67.
3. Rupprecht, J. K.; Hui, Y.-H.; McLaughlin, J. L. *J. Nat. Prod.* **1990**, *53*, 237-278.
4. Ahammadsahib, K. I.; Hollingworth, R. M.; McGovren, P. J.; Hui, Y.-H.; McLaughlin J. L. *Life Sciences* **1993**, *53*, 1113-1120.
5. Lewis, M. A.; Arnason, J. T.; Philogene, B. J.; Rupprecht, J. K.; McLaughlin, J. L. *Pestic. Biochem. Physiol.* **1993**, *45*, 15-23.

6. Londershausen, M.; Leicht, W.; Lieb, F.; Moeschler, H.; Weiss, H. *Pestic. Sci.* **1991**, *33*, 427-438.
7. Degli Esposti, M.; Ghelli, A.; Ratta, M.; Cortes, D. *Biochem. J.* **1994**, *301*, 161-167.
8. Hollingworth, R. M.; Ahammadsahib, K. I.; Gadelhak, G.; McLaughlin, J. L. *Biochem. Soc. Trans.* **1994**, *22*, 230-233.
9. Morre, D. J.; de Cabo, R.; Farley, C.; Oberlies, N. H.; McLaughlin, J. L. *Life Sciences* **1995**, *56*, 343-348.
10. Wolvetang, E. J.; Johnson, K. L.; Krauer, K.; Ralph, S. J.; Linnane, A. W. *FEBS Lett.* **1994**, *339*, 40-44.
11. Rupprecht, J. K.; Chang, C. -J.; Cassady, J. M.; McLaughlin, J. L.; Mikolajczak, J. L.; Weisleder, D. *Heterocycles* **1986**, *24*, 1197-1201.
12. Zhao, G.-X.; Hui, Y.-H.; Rupprecht, J. K.; McLaughlin, J. L.; Wood, K. V. *J. Nat. Prod.* **1992**, *55*, 347-356.
13. Zhao, G.-X.; Miesbauer, L. R.; Smith, D. L.; McLaughlin, J. L. *J. Med. Chem.*. **1994**, *37*, 1971-1976.
14. Zhao, G.-X; Ng, J. H.; Kozlowski, J. F.; Smith, D. L.; McLaughlin, J. L. *Heterocycles* **1994**, *38*, 1897-1908.
15. Zhao, G.-X; Rieser, M. J.; Hui, Y.-H.; Miesbauer, L. R.; Smith, D. L.; McLaughlin, J. L. *Phytochemistry.* **1993**, *33*, 1065-1073.
16. McAlpine, J. B., Abbott Laboratories, personal communication.
17. Rieser, M. J.; Hui, Y.-H.; Rupprecht, J. K.; Kozlowski, J. F.; Wood, K. V.; McLaughlin, J. L.; Hanson, P. R.; Zhuang, Z.; Hoye, T. R. *J. Am. Chem. Soc.* **1992**, *26*, 10203-10213.
18. Hoye, T. R.; Hanson, P. R.; Hasenwinkel, L. E.; Ramirez, E. A.; Zhuang, Z. *Tetrahedron Lett.* **1994**, *35*, 8525-8528.
19. Hoye, T. R.; Hanson, P. R.; Hasenwinkel, L. E.; Ramirez, E. A.; Zhuang, Z. *Tetrahedron Lett.* **1994**, *35*, 8529-8532.
20. Ohtani, I.; Kusumi, T., Kashman, Y.; Kakisawa, H. *J. Am. Chem. Soc.* **1991**, *113*, 4092-4096.
21. Dale, J. A.; Mosher, H. S. *J. Am. Chem. Soc.* **1973**, *95*, 512-520.
22. Dale, J. A.; Mosher, H. S. *J. Org. Chem.* **1973**, *38*, 2143.
23. Jolad, S. D.; Hoffmann, J. J.; Cole, J. R.; Barry, C.E.; Bates, R. B.; Linz, G. S.; Konig, W. A. *J. Nat. Prod.* **1985**, *48*, 644-645.
24. Born, L.; Lieb, F.; Lorentzen, J. P.; Moeschler, H.; Nonfon, M.; Sollner, R.; Wendisch, D. *Planta Med.* **1990**, *56*, 312-316.
25. Araya, H.; Hara, N.; Fujimoto, Y.; Srivastava, A.; Sahai, M. *Chem. Pharm. Bull.* **1994**, *42*, 388-391.
26. Sahai, M.; Singh, S.; Singh, M.; Gupta, Y. K.; Akashi, S.; Yuji, R.; Hirayama, K.; Asaki, H.; Araya, H.; Hara, N.; Eguchi, T.; Kakinuma, K.; Fujimoto, Y. *Chem. Pharm. Bull.* **1994**, *42*, 1163-1174.
27. Hoye, T. R.; Zhuang, Z.-P. *J. Org. Chem.* **1988**, *53*, 5578.
28. Hoye, T. R.; Suhadolnik, J. C. *J. Am. Chem. Soc.* **1987**, *109*, 4402.
29. Nishioka, S.; Araya, H.; Murasaki, C.; Sahai, M.; Fujimoto, Y. *Nat. Prod. Lett.* **1994**, *5*, 117-121.
30. McLaughlin, J. L. "Methods in Plant Biochemistry", Vol. 6, Ed. by K. Hostettmann, Academic Press, London, **1991**, pp. 1-35.
31. Meyer, B. N.; Ferrigni, N. R.; Putnam, J. E.; Jacobsen, L. B.; Nichols, D. E.; McLaughlin, J. L. *Planta Med.* **1982**, *45*, 31.

(*Received in USA* 2 *March* 1995; *accepted* 5 *May* 1995)